ANNALS OF MEDICINE, 2016
VOL. 48, NO. 8, 652–668
http://dx.doi.org/10.1080/07853890.2016.1219455

Taylor & Francis
Taylor & Francis Group

ORIGINAL ARTICLE

OPEN ACCESS

The brain-tumor related protein podoplanin regulates synaptic plasticity and hippocampus-dependent learning and memory

Ana Cicvaric[a], Jiaye Yang[a], Sigurd Krieger[b], Deeba Khan[a], Eun-Jung Kim[c], Manuel Dominguez-Rodriguez[a], Maureen Cabatic[a], Barbara Molz[d], Juan Pablo Acevedo Aguilar[a], Radoslav Milicevic[a], Tarik Smani[e], Johannes M. Breuss[f], Dontscho Kerjaschki[b], Daniela D. Pollak[a], Pavel Uhrin[f] and Francisco J. Monje[a]

[a]Department of Neurophysiology and Neuropharmacology, Center for Physiology and Pharmacology, Medical University of Vienna, Vienna, Austria; [b]Clinical Institute of Pathology, Medical University of Vienna, Vienna, Austria; [c]Paik Institute for Clinical Research, Inje University College of Medicine, Busan, Republic of Korea; [d]Psychology University of York, Heslington York, UK; [e]Grupo de Fisiopatología Cardiovascular, Instituto de Biomedicina de Sevilla (IBiS), Hospital Universitario Virgen del Rocío/CSIC/Universidad de Sevilla, Seville, Spain; [f]Department of Vascular Biology and Thrombosis Research, Center for Physiology and Pharmacology, Medical University of Vienna, Vienna, Austria

ABSTRACT

Introduction: Podoplanin is a cell-surface glycoprotein constitutively expressed in the brain and implicated in human brain tumorigenesis. The intrinsic function of podoplanin in brain neurons remains however uncharacterized.

Materials and methods: Using an established podoplanin-knockout mouse model and electrophysiological, biochemical, and behavioral approaches, we investigated the brain neuronal role of podoplanin.

Results: *Ex-vivo* electrophysiology showed that podoplanin deletion impairs dentate gyrus synaptic strengthening. *In vivo*, podoplanin deletion selectively impaired hippocampus-dependent spatial learning and memory without affecting amygdala-dependent cued fear conditioning. *In vitro*, neuronal overexpression of podoplanin promoted synaptic activity and neuritic outgrowth whereas podoplanin-deficient neurons exhibited stunted outgrowth and lower levels of p-Ezrin, TrkA, and CREB in response to nerve growth factor (NGF). Surface Plasmon Resonance data further indicated a physical interaction between podoplanin and NGF.

Discussion: This work proposes podoplanin as a novel component of the neuronal machinery underlying neuritogenesis, synaptic plasticity, and hippocampus-dependent memory functions. The existence of a relevant cross-talk between podoplanin and the NGF/TrkA signaling pathway is also for the first time proposed here, thus providing a novel molecular complex as a target for future multidisciplinary studies of the brain function in the physiology and the pathology.

KEY MESSAGES

- Podoplanin, a protein linked to the promotion of human brain tumors, is required *in vivo* for proper hippocampus-dependent learning and memory functions.
- Deletion of podoplanin selectively impairs activity-dependent synaptic strengthening at the neurogenic dentate-gyrus and hampers neuritogenesis and phospho Ezrin, TrkA and CREB protein levels upon NGF stimulation.
- Surface plasmon resonance data indicates a physical interaction between podoplanin and NGF. On these grounds, a relevant cross-talk between podoplanin and NGF as well as a role for podoplanin in plasticity-related brain neuronal functions is here proposed.

ARTICLE HISTORY
Received 23 May 2016
Revised 14 July 2016
Accepted 25 July 2016

KEYWORDS
Podoplanin; Ezrin; dentate gyrus; hippocampus; neuron; synaptic plasticity; memory; nerve growth factor

Introduction

Podoplanin (1–3) (also known as aggrus, glycoprotein 36, PA2.26 antigen, T1-alpha) is a cell-surface transmembrane sialomucin-like glycoprotein of ~40 kDa present in humans and other species and constitutively expressed in the developing and adult mammalian brain (4). Podoplanin has recently emerged as a promotor of malignant human brain cancer (4) and recent *in vitro* studies in non-neuronal HEK293T and MDCK cells have also identified podoplanin as a substrate of presenilin-1/gamma-secretase (5), which is causally linked to familial Alzheimer's disease (6–9). In non-neuronal cells, podoplanin has been additionally implicated in the regulation of cell morphology and

CONTACT Dr Francisco J. Monje francisco.monje@meduniwien.ac.at Department of Neurophysiology and Neuropharmacology, Center for Physiology and Pharmacology, Medical University of Vienna, Schwarzspanierstrasse 17, A-1090 Vienna, Austria

growth factor signaling (4,10,11). However, neither the involvement of podoplanin in memory-related hippocampal synaptic plasticity functions, nor the possible functional association of podoplanin with brain growth factor signaling have been previously described. To the best of our knowledge, the constitutive role of podoplanin in the mammalian brain neuron remains thus far completely unknown.

Here, we combined overexpression experiments using primary-dissociated hippocampal neurons obtained from wild-type mice with the use of a podoplanin knockout mice (podoplanin−/−), previously described in the context of vascular system studies (12), as experimental models to learn about the physiological importance of podoplanin in the mammalian central nervous system. We provide the first experimental evidence indicating that podoplanin is implicated in the regulation of brain neuronal outgrowth, synaptic plasticity, and hippocampus-dependent learning and memory. Also for the first time, we describe that podoplanin can physically interact with NGF, a neurotrophin importantly implicated in the regulation of hippocampus-mediated memory storage (13), in the pathophysiology of brain tumors (14,15) and in Alzheimer's disease (16–19). Our data propose podoplanin as a novel molecular component of the cellular machinery regulating neuritogenesis and memory-related synaptic plasticity through a mechanism involving physical interaction with NGF and modulation of p-Ezrin, TrkA, and CREB protein levels.

Materials and methods

Animals

Podoplanin−/− mice and wild-type littermates in 129S/v: Swiss background were obtained by crossing of heterozygous mice. Animals were housed in a temperature-controlled colony room (22 ± 1 °C) and provided with food and water *ad libitum*. Mice were maintained on a 12-h light/dark cycle with lights on at 6:00 a.m. and with 200-220 lux inside the cages. Animal experiments described in this study were approved by the Bundesministerium für Wissenschaft, Forschung und Wirtschaft (BMWFW-66.009/0201-WF/II/3b/2014) and carried out according to EU-directive 2010/63/EU.

Preparation of the podoplanin-overexpression construct

The mouse podoplanin cDNA was obtained by PCR amplification from total cDNA prepared by reverse transcription of RNA derived from a mouse brain and using podoplanin specific primers 5′-CAA CAA GCT TAA GAT GTG GAC CGT GCC AG-3′ and 5′-TAG CAA GCT TGG GCG AGA ACC TTC CAG AAA TC-3′ containing engineered HindIII sites. The HindIII restricted fragment was subsequently cloned into HindIII digested pEGFP-N1 (Clontech, Takara Bio Europe, Saint-Germain-en-Laye, France) vector and the absence of mutations in podoplanin cDNA was verified by sequencing. Plasmidic vectors were amplified under endotoxin-free conditions and used for transfection.

Hippocampal neuronal cultures and morphological analysis

Hippocampal tissue from newborn wild type and podoplanin−/− pups (Postnatal day PND1-3) was used to prepare cultures of primary neurons following standardized protocols described before (20). Cultures and overexpression experiments were conducted in triplicates and a number of 8–23 cells per group were examined at each time point. Transfections were performed using the Calcium Phosphate method kit (Invitrogen, Thermo Scientific, Vienna, Austria), following the recommendations of the supplier. Average lengths of neuritic branches were evaluated using confocal microscopy via an Axiovert 200M (Zeiss, Graz, Austria) microscope and analyzed using ImageJ software (http://rsbweb.nih.gov/ij/) as described before (20).

Preparation of hippocampal slices

Tissue preparation and extracellular electrophysiological recordings were performed *ex vivo* in hippocampal slices following protocols previously described (20,21) with minor modifications. Briefly, nine animals per group (wild-type and podoplanin−/− mice, 8–10 weeks old) were deeply anesthetized with isoflurane and sacrificed by rapid cervical dislocation and swift sharp-blade decapitation. Brains were quickly removed and rapidly immersed in a frosty aCSF containing (in mM): 125 NaCl, 2.5 KCl, 25 $NaHCO_3$, 2 $CaCl_2$, 1 $MgCl_2$, 25 D-glucose, and 1.25 NaH_2PO_4 (all purchased from Sigma-Aldrich, Vienna, Austria). Resection of hippocampi was conducted while maintaining the brain submerged in aCSF. During all working conditions, aCSF was constantly bubbled with a carbogen gas mixture (95% oxygen, 5% carbon dioxide). Transverse hippocampal slices (400 μm thickness) were obtained using a McIlwain Tissue Chopper (Mickle Laboratory Engineering, Gomshall, Surrey, UK). Slices were then

quickly transferred to a customized nylon-mesh recovery chamber submerged in 200 mL of aCSF and maintained at 28 ± 2 °C. Slices recovered for at least 1 h before electrophysiological recordings.

PCR

For the determination of podoplanin levels by real-time PCR, total RNA from different organs of wild-type mice was isolated using the Trizol reagent (Life Technologies, Vienna, Austria). Upon reverse transcription [using MuLV-reverse transcriptase, RNAse inhibitor and oligo dT16 primers (Life Technologies, Vienna, Austria)], real-time PCR was conducted in a StepOnePlus Real-Time PCR Cycler (Life Technologies, Vienna, Austria) using FastStart SYBR Green Master Mix (Life Technologies, Vienna, Austria). Expression levels of podoplanin were determined using forward 5′-GTG ACC CCA GGT ACA GGA GA-3′ and reverse 5′-GCT GAG GTG GAC AGT TCC TC-3′ primers (167-bp amplicon) and by normalization to the expression of β2-microglobulin gene amplified by 5′-ATT CAC CCC CAC TGA GAC TG-3′ and 5′-TGC TAT TTC TTT CTG CGT GC-3′ primers (193-bp amplicon).

Western blotting

For Western blotting assays, cultured cells and brain tissue from adult animals (8–10 weeks old) were homogenized using a freshly prepared protein lysis buffer containing (in mM) 10 Tris-HCl, 150 NaCl, 10 NaF, 10 Na_3VO_4, 1 EDTA, 5 $Na_4P_7O_2$, and 1% SDS, 0.5% Triton ×100, as well as protease inhibitor cocktail (Complete™, Roche Diagnostics, Mannheim, Germany). Electrophoresis of samples was performed on 10% SDS-PAGE gels. Proteins were transferred to a polyvinylidine fluoride (PVDF) membrane, blocked for 1 h at room temperature, and incubated overnight in primary antibody solution at 4 °C. Membranes were then washed and incubated with corresponding secondary antibodies solution for 1 h at room temperature. Chemiluminescent detection was performed using a FluorChem HD2 system (Alpha Innotech, San Leandro, CA). Images were quantified using ImageJ software and densitometric values normalized to levels of indicated housekeeping protein. Primary antibodies used were: Abcam, Cambridge, UK (anti-podoplanin, ab11936; anti-synaptophysin, ab32127, anti-synaptotagmin I, ab10104 and anti-phospho-Ezrin, ab 47293), Cell Signaling Technology Inc., Danvers, MA (anti-TrkA, 2505, anti-CREB, 9197), Millipore Merck GesmbH, Vienna, Austria (anti-Ezrin, 07-130), and AbFrontier, Seoul, South Korea (anti- β-tubulin, LF-MA20056).

Immunohistochemistry

Immunohistochemistry using tissue from adult animals (8–10 weeks old) was performed as described elsewhere (22) with minor modifications. Briefly, frozen sections (30 μm thickness) of intracardially perfused (4% PFA/PBS) adult mouse brains were cut using a cryostat (Leica CM1950, Leica Mikrosysteme Handelsges.m.b.H., Vienna, Austria). Following 1 h blocking at room temperature, free-floating brain sections were incubated overnight at 4 °C with anti-podoplanin antibody (sc-134483, Santa Cruz Biotechnology Inc, Heidelberg, Germany, 1:200 dilution) and subsequently incubated with an anti-rabbit secondary antibody (Abcam, Cambridge, UK, 1:500) for 1 h. Transverse sections were examined under a conventional fluorescence confocal microscope.

Electrophysiology

The measurements of miniature excitatory postsynaptic currents (mEPSCs) were conducted in the whole-cell configuration of the patch clamp technique using primary-cultured hippocampal neurons (10 DIV) essentially as previously described (20). Briefly, recordings were conducted at room temperature (22 ± 2 °C) with neurons clamped at a holding potential of −70 mV. Currents were measured using the Patchmaster and analyzed offline with FitMaster software packages (Heka Electronics, Lambrecht/Pfalz, Germany). The bath solution contained 140 mM NaCl, 6 mM KCl, 3 mM $CaCl_2$, 2 mM $MgCl_2$, 25 mM glucose, and 10 mM Hepes (pH = 7.4 adjusted with NaOH). In all experiments, 0.5 μM tetrodotoxin was included to inhibit voltage-gated sodium channel conductance. Bicucullinemethiodide (30 μM) was also used to suppress inhibitory currents. Recording pipettes, from borosilicate glass capillaries, were pulled in a horizontal puller (Sutter Instrument, Novato, CA) yielding tip resistances of 2–4 MΩ when filled with a solution containing 140 mM KCl, 1.5 mM $CaCl_2$, 10 mM EGTA, 10 mM Hepes, and 2 mM Mg-ATP (pH 7.3 adjusted with KOH). Events with amplitudes lower than 5 pA and events with a rise time higher than 5 ms were excluded from analysis. For dentate gyri recordings in hippocampal slices, the middle molecular layer pathway was stimulated (0.1 ms duration, 0-6 V amplitude) via a custom-made bipolar tungsten electrode insulated to the tip (50 μm tip diameter) and using an ISO-STIM 01D isolator stimulator (NPI Electronics, Tamm, Germany). Evoked fEPSPs were recorded at the MPP area using aCSF-filled glass micropipettes (2–4 MΩ) located about 400 μm away from the stimulating

electrode, as previously described (21). Recordings at CA3-Schaffer Collateral-CA1 synaptic regions were conducted as described before (20). Input/output curves were obtained by delivering increasing pulses of voltage (100 μs in duration) between 0 and 6 V with a delta of 1 V and 10 s between pulses. The strength of synaptic transmission was determined from the decaying slope of recorded fEPSPs. For LTP, basal synaptic transmission (baseline) was examined for at least 20 min by recording stable fEPSPs in response to voltage pulses that elicited 40% of the maximal fEPSP (100 μs; 0.03 Hz). Next, an electrical stimulation protocol was applied (5 trains/100 Hz, 100 μs/pulse, 4 s between trains) and measurements returned to those of baseline conditions for at least one additional hour. Synaptic potentiation was determined by examining the temporal course of the initial decaying fEPSPs slopes following electrical stimulation, normalized to baseline values. Recordings were made using an AxoClamp-2B amplifier (Bridge mode) and a Digidata-1440 interface (Axon Instruments, Molecular Devices, Berkshire, UK). Data were analyzed using the pClamp-10 Program software (Molecular Devices, Berkshire, UK).

Behavioral analysis

Male adult podoplanin−/− and wild-type littermate controls (10–12 animals per group, 8–10 weeks old) were used for behavioral experiments. Sample sizes were similar to those reported in previous studies (20) with the aim to reduce animal suffering and keep the number of animals used at the minimum level. All animals were naïve, i.e. without any prior manipulation, at the onset of experiments. Animals were single-housed in standard transparent laboratory cages one week prior to the start of behavioral experiments, which were all carried out during the light-phase of the light/dark cycle. Behavioral analyses were carried out by an experimenter blinded to the experimental groups.

Morris water maze

The Morris water maze followed a previously described set up (20). The spatial acquisition phase consisted of three trials per day (120 s, each) over the course of three days. Using distal cues, mice had to find a submerged platform (in the target quadrant) in the testing pool. The water in the testing pool was made opaque by non-toxic white paint (Viewpoint®, Lyon, France). Mice were tracked from above the experimental setup by a camera coupled to computational tracking software (Videotrack [02-WATERMAZE-NSHD-LBW] Viewpoint®, Lyon, France). The probe trial consisted of one session (60 s) without the submerged platform. Time spent in the target quadrant as compared to the time spent in the other three quadrants was evaluated for the first 15 s of the probe trial.

Rota rod

Rota Rod (USB Rota Rod "SOF-ENV-57X", Medassociates Inc., St. Albans, VT), was performed in triplicate for each mouse in 5 min sessions in order to evaluate motor coordination following a published procedure (23).

Fear conditioning

Fear conditioning paradigm was performed as described before (24). Briefly, mice were tested in an external sound-isolated chamber (Medassociates Inc., St. Albans, VT) provided with an electrically conductive metal-grid floor for stimuli delivery. Following 120 s of habituation in the test chamber, mice received two consecutive tone stimuli (60 s interval) of 30 s (75 db, rise time 50 ms). 2 s before the end of each tone stimulus, a mild 0.6 mA foot shock (2 s) was delivered. Chambers were thoroughly cleaned with 70% ethanol after each subject session to remove olfactory signaling inputs. Training sessions were repeated for 2 days and 24 h later animals were examined for contextual fear memory retention in the familiar context for 5 min. Mice behavior was recorded and analyzed using the Video Freeze® Software (Med Associates Inc., Fairfax, VT). Cued fear memory retention was tested more than 4 h later in chambers with white flat-floor provided with a completely different odor. Mice were placed in these chambers and, 60 s later, the cue was presented during 30 s. Freezing behavior before and during tone presentation was measured. Data are shown as mean ± SEM of freezing response (% of total time).

Surface plasmon resonance

All experiments were performed on a BIACORE instrument (BIAcore, Uppsala, Sweden). In brief, CM5 sensor chips for standard amino coupling procedure were used. For activation of the carboxymethylated dextran surface, equal volumes of 0.1 M N-hydroxysulfosuccinimide and 0.4 M 1-ethyl-3-(3-diethylaminopropyl) carbodiimide were mixed, and 35 μl were injected. Human podoplanin extracellular domain/Fc chimera (PDPN/Fc) was expressed in HEK-293 cells and protein G sepharose affinity purified from cell culture

supernatants. PDPN/Fc in 10 mM sodium acetate/pH 4.0 at a concentration of 30 μg/mL was injected for coupling on one of the two channels of the sensor chip. The coating efficiency ranged from 6000 to 8000 response units covalently bound PDPN/Fc corresponding to 6 to 8 ng of bound protein. Unreacted N-hydroxysulfosuccinimide-ester groups were deactivated by injecting a 35 μl pulse of 1 M ethanolamine hydrochloride. On the second channel, the dextran surface was immediately saturated with ethanolamine after activation, and was used as response reference. Changes in resonance recorded in this channel were subtracted from the one with coupled PDPN/Fc to account for bulk effects and nonspecific binding. All experiments were carried out at 20 °C using running buffer HBS-P (0.01 M Hepes pH 7.4/0.15 M NaCl/0.005% Surfactant P20) at a flow rate of 5 μl/min. Recombinant carrier-free human βNGF (R&D Systems, Minneapolis, MN, 256-GF-100/CF) was used to test the interaction of PDPN and NGF. One micro molar concentrations of NGF were injected onto the sensor chip at a flow rate of 5 μl/min to measure association and dissociation phases of the interaction. Between the successive measurements, the surface was regenerated with pulses of 1% Heparin in phosphate buffered saline until the baseline reached the original value. To test the specificity of the interaction of PDPN and NGF, excessive amounts (e.g. 2 μg) of human Fc fragments lacking the extracellular domain of PDPN were pre-incubated with 50 μl aliquots of 1 μM NGF for 10 min to block possible unspecific binding sites of NGF to the Fc portion of the PDPN/Fc chimera. Recombinant carrier-free myostatin/GDF-8 (RnDSystem, 788-G8-010/CF) was identified in former screens as a PDPN non-interacting factor and was therefore used as negative control and to exclude bulk response effects. Sensorgrams were fitted to a single site binding model (1:1 Langmuir binding), using the numerical integration functions of the BIAevaluation 3.1 software package (Biacore; GE Healthcare Europe GmbH, Vienna, Austria). The forward and reverse rate constants (k_a and k_d) were determined and the dissociation constant (k_D) was estimated by the steady-state affinity binding model, also provided by the BIAevaluation 3.1 software.

Statistical evaluation

All statistical analyses were carried out using BioStat 2009 professional software (AnalystSoft Inc., Walnut, CA). Comparisons between two groups were analyzed by unpaired, two-tailed Student's *t*-test. For Western blot analysis, investigating the effects of NGF in podoplanin−/− and wild-type mice, unpaired, two-tailed Student's *t*-test or two-way ANOVA (treatment × genotype) was employed. LTP in podoplanin−/− and wild-type mice was evaluated by mixed-model repeated measure ANOVA. $p < 0.05$ was considered statistically significant in all instances.

Results

Podoplanin is profusely expressed in the neurogenic dentate gyrus

Brain patterns of protein expression differ significantly depending on individual mouse strain, resulting in important differences in terms of molecular signaling, behavioral and cognitive functions (25–28). We therefore first corroborated the expression pattern of podoplanin in the adult brain of the specific mice strain used in this research (12). RT-PCR assay indicated abundant presence of podoplanin transcripts in the brains of wild-type mice and comparatively lower levels in all the other tissues tested (Figure 1(a,b)). The distribution of podoplanin in the brain was also verified by immunohistochemistry. In agreement with previous observations (22), our data showed a clear signal for podoplanin in cortex and a markedly profuse expression density in cells of the hippocampal dentate gyrus (Figure 1(c)). Immunoblotting (Figure 1(d)) confirmed the expression of podoplanin in mature wild-type adult mouse hippocampus and lack of the protein in the podoplanin knockout mouse used in this research (see below).

Podoplanin deletion selectively impairs long-term synaptic plasticity in the hippocampal dentate gyrus

The profuse expression of podoplanin in the hippocampus suggested a potential implication of podoplanin in hippocampal synaptic plasticity. To examine this possibility *ex vivo*, we prepared hippocampal slices from wild-type and podoplanin−/− mice and performed electrophysiological recordings of fEPSPs ("Materials and methods" section) in order to examine the properties of long-term synaptic potentiation (LTP). We first examined the properties of long-term synaptic plasticity in CA3-Schaffer Collateral-CA1 pathway of the hippocampus. Podoplanin−/− slices presented with memory-related LTP in CA3-Schaffer Collateral-CA1 pathway synapses that were indistinguishable from those from wild-type animals (Figure 2(a)). We next examined the properties of long-term synaptic

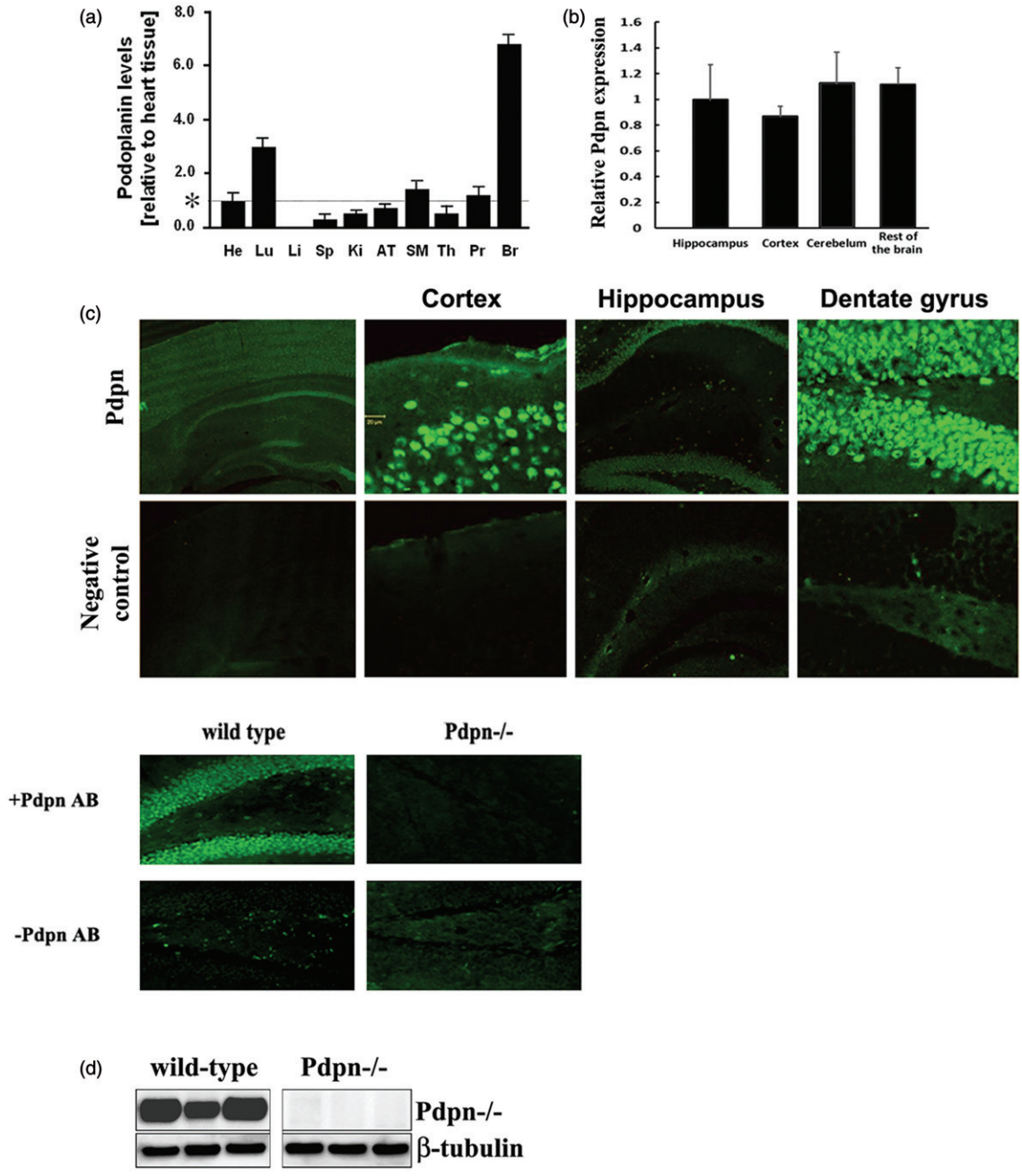

Figure 1. Podoplanin is expressed in the mouse brain. (a) qPCR examinations in adult (8–10 weeks old) wild-type mouse tissues (n = 3 animals) indicated a salient presence of podoplanin in the brain. Transcription levels from triplicate experiments were normalized to values obtained from podoplanin in the heart, for descriptive proposes, as indicated by an asterisk. He = heart, Lu = lung, Li = liver, Sp = spleen, Ki = kidney, AT = adipose tissue, SM = skeletal muscle, Th = thymus, Pr = prostate, Br = total brain. (b) In a different experiment, qPCR analysis further verified the presence of podoplanin mRNAs in different areas across the brain relative to the hippocampus of 8–10 weeks old wild-type mice (n = 3). (c) Immunohistochemical staining of brain sections obtained from adult wild type mice showed a clear signal for podoplanin (upper) and no signal in negative controls where primary antibody was omitted (lower). Objective magnifications -from left to right- are 4×, 20×, 20×, and 40× for upper and lower pictures. Consistent results were found when the podoplanin antibody was used on brain sections obtained from the podoplanin knock out (Pdpn−/−) mice (lower pictures). (d) Western blot assay exclusively using hippocampal tissue from wild-type mice corroborated the expression of podoplanin. No signal was detected in hippocampal tissue from podoplanin−/− mice (right). Histograms data are displayed as mean ± SEM.

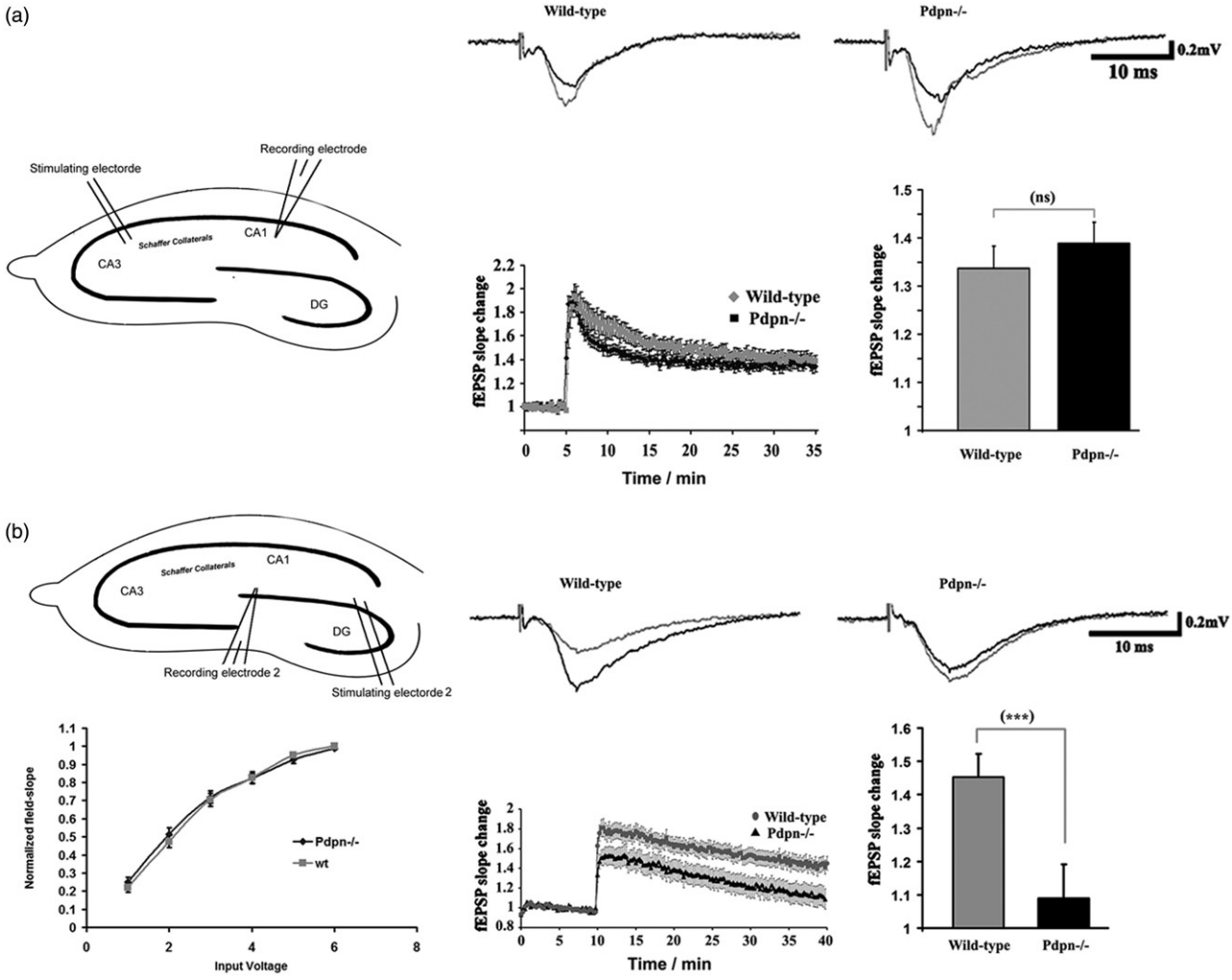

Figure 2. Podoplanin deletion selectively impairs long-term synaptic plasticity in the hippocampal dentate gyrus. (a) Comparative examinations of LTP in CA3-Schaffer collateral-CA1 synapses (inset cartoon in left represents the positioning of stimulating and recording electrodes) of slices obtained from wild-type and podoplanin−/− mice (n = 9 animals per group). (b) No differences in basal synaptic transmission (left) was detected at the dentate gyrus (inset cartoon in left represents the positioning of stimulating and recording electrodes) in hippocampal slices from podoplanin−/− and control wild-type mice as examined by input/output protocols. Right, representative fEPSPs traces (upper insets); temporal courses (lower chart plot) of averaged field-postsynaptic-potential-slopes; and corresponding bar graphs of the end-time points (right) of data obtained before and after application of electrical stimulation inducing long-term-potentiation (LTP) in the dentate gyrus. A mixed-model repeated measure ANOVA indicated no main effect of genotype ($p > 0.05$), a highly significant main effect of time ($F_{158,82} = 57.05$, $p < 0.0001$) and a significant interaction between the two factors ($F_{52,16} = 3.45$, $p < 0.0001$). Data revealed significant differences in the later phases of synaptic potentiation only in the dentate gyrus. Data are displayed as mean ± SEM. ***($p \leq 0.001$), ns ($p > 0.05$).

plasticity in the dentate gyrus, the region of the hippocampus with the higher density of cells expressing podoplanin. Whereas no differences in basal synaptic transmission were observed between podoplanin−/− and control wild-type mice, we observed that high-frequency stimulation protocols known to induce LTP ("Materials and methods" section) resulted in both hampered induction of post-synaptic strengthening and significantly weaker persistence of the induced potentiation in slices from podoplanin−/− mice compared to those from their control wild-type counterparts (Figure 2(b)).

In vivo *deficiency of podoplanin impairs hippocampus-dependent spatial memory*

The profuse expression of podoplanin in the hippocampus, a structure critical for spatial memory, together with the impairment in long-term synaptic plasticity in the hippocampus resulting from podoplanin deletion, prompted us to further explore the possible involvement of podoplanin in the formation and maintenance of spatial memory *in vivo*. To this aim, wild-type controls and podoplanin−/− mice were subjected to the Morris water maze, a model

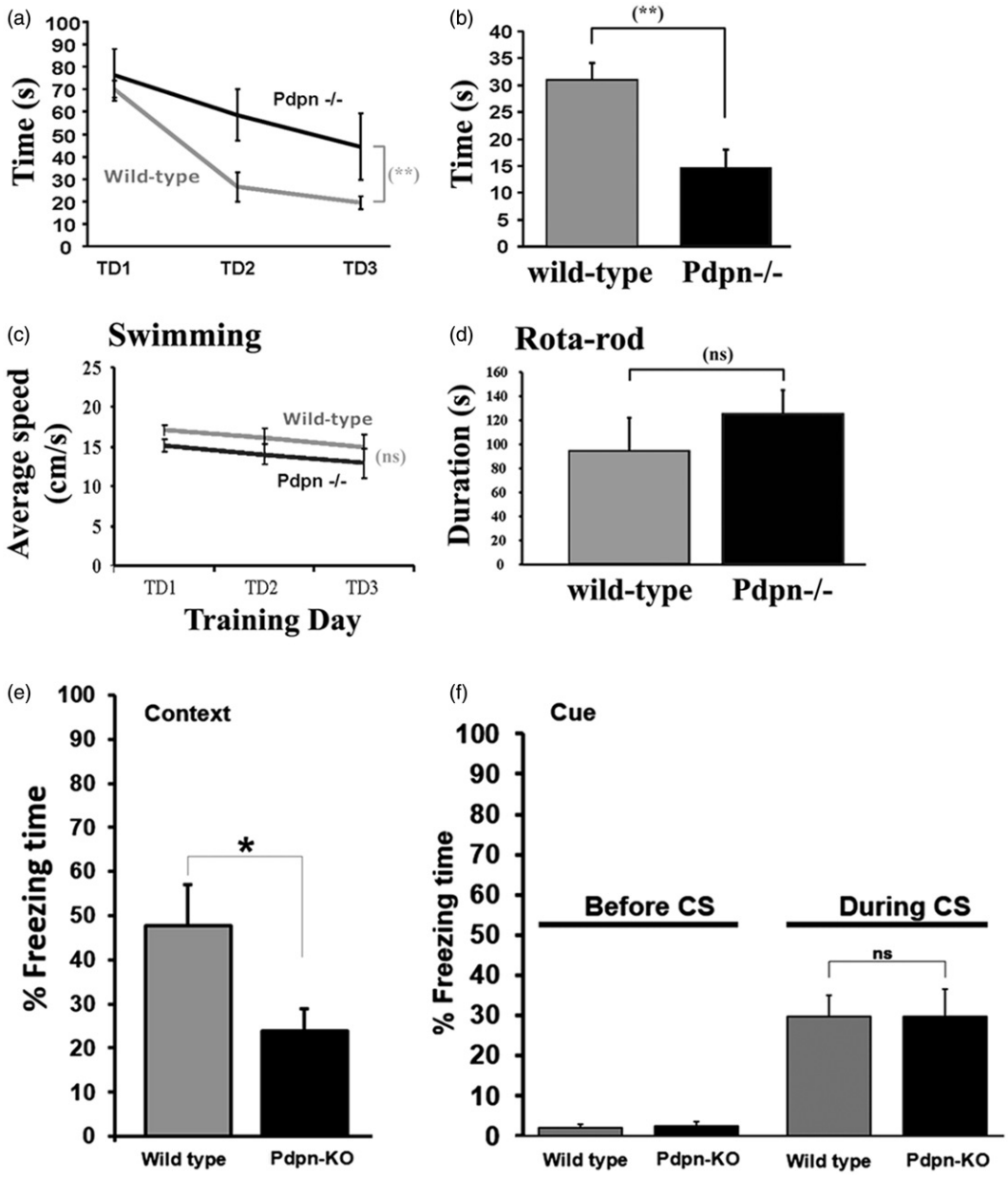

Figure 3. *In vivo* lack of podoplanin impairs hippocampus-dependent spatial learning and memory. (a) The latency to reach the hidden platform in the Morris water maze during three days of training (TD 1-3) is displayed as average of three trials per day. Escape latency was significantly higher in podoplanin−/− mice as compared to wild-type controls on TD 2 and TD 3. (b) During the probe trial, implemented to examine the retention in memory of the behavioral tasks, the percentage of time spent in the target quadrant (original location of the platform during training) was lower for podoplanin−/− animals compared to that of wild-type mice. No significant differences were observed either in the average speed of swimming (c) or in the performance on the Rota Rod test (d) between wild-type and podoplanin−/− mice. Data are displayed as mean ± SEM. **($p \leq 0.01$), ns ($p > 0.05$). (e) Podoplanin−/− mice exhibited a statistically significant reduction in the time of freezing when hippocampus-dependent contextual fear-conditioning was examined. (f) Podoplanin−/− mice present with amygdala-dependent cued fear conditioning indistinguishable from that from wild-type counterparts.

widely used to study hippocampus-dependent spatial learning and memory. Examination of the time required for the learning of the experimental task revealed a significant memory deficit in podoplanin−/− mice, evidenced by the increased time needed to reach the hidden platform (Figure 3(a)). Twenty-four hours after the last training trial, a probe trial was conducted in which the time spent in the quadrant which originally contained the platform was used as an indicator of hippocampus-dependent spatial-memory retrieval (“Materials and methods” section). As expected, control mice

consistently displayed a significant preference in searching for the platform precisely in the target quadrant area where the platform used to be located (circa 50% of total probe trial time), as shown in Figure 3(b). In contrast, podoplanin−/− mice spent comparable times for all quadrants indicating a deficiency in hippocampus-dependent spatial-memory retrieval. No significant differences with respect to swimming speeds and performance on the Rota rod were detected between wild-type controls and podoplanin−/− mice (Figure 3(c,d)).

To further study the potential involvement of podoplanin in hippocampus-mediated memory functions *in vivo* using a completely different behavioral approach, we decided to examine fear conditioning, a form of learned fear in which the animals learn to associate an initially innocuous stimuli with the presence of threatening noxious events. We observed that podoplanin−/− mice presented with significantly impaired hippocampus-dependent contextual fear-conditioning, compared to wild-type controls, whereas no significant differences were detected when amygdala-dependent cued fear conditioning was examined.

Survivor podoplanin−/− mice don't exhibit other distinctive phenotypic abnormalities

Previous reports from vascular physiology studies showed that genetic elimination of podoplanin results in two major phenotypes. First, a large proportion of podoplanin−/− mice die right after birth due to vascular cardiac and respiratory failures (4,12). Second, here we and others have observed that a significant number of podoplanin knockout mice survive with phenotypic abnormalities that recede and resolve few days after birth (4,12). For this study, we used surviving podoplanin−/− mice previously described in the context of extracerebral studies (12). We examined several standard phenotypical factors in these podoplanin−/− mouse line including behavioral, molecular biochemical and body and brain anatomical features in order to explore for the possible existence of salient abnormalities potentially attributable to developmental alterations and that could act as confounding factors during this study. In agreement with previous reports (12), we observed that surviving podoplanin−/− animals reached adulthood having normal body weights and body lengths (Figure 4(f-g)), normal life spans, normal fertility and did not present with pulmonary or other macroscopically observable abnormalities that otherwise would have resulted in early lethality. We examined the gross morphological characteristics of the podoplanin−/− and wild-type mice and did not observe differences in gross structural appearance of the body or brains for newborn PND-1-3 (Figure 4(a)), later PND 10-15 (Figure 4(b)), or mature adult (Figure 4(c), middle and left panels) animals.

Similarly, gross histological examination of the structural and layer arrangements of the cortex, hippocampus and cerebellum did not reveal neuroarchitectural abnormalities in mature adult podoplanin−/− mice compared to wild-type littermates (Figure 4(c), right panels). Whereas we cannot exclude that a more detailed analysis could reveal subtle alterations, which have not been observed using the methods applied herein, our observations show that the brains of surviving podoplanin knockout mice do not present with gross abnormalities throughout life. Moreover, while one or two mild anomalies in brain vascular morphology were found in some PND1-3 podoplanin−/− pups (Figure 4(a)), these anomalies were very small in size, not widespread and randomly localized in superior-caudal areas of the cortex (Figure 4(a)). However, no detectable vascular anomalies were observed in the cortex, hippocampus or other gross brain areas of PND10-15 (Figure 4(b)) or mature adult (Figure 4(c)) podoplanin−/− mice. Furthermore, we isolated hippocampal tissue from adult mice and examined by Western blotting the levels of synaptotagmin I and synaptophysin, two basic proteins associated with neuronal outgrowth and the synaptic function. No significant differences were found between wild-type and podoplanin−/− sample tissues (Figure 4(d,e)).

Overexpression of podoplanin in primary-cultured neurons enhances synaptic activity and neuritic outgrowth

In order to independently examine the competence of podoplanin to influence the molecular machinery regulating the morphofunctional properties of brain neurons, we examined the effects of podoplanin overexpression on the electrophysiological and morphological properties of primary-cultured hippocampal neurons obtained from newborn PND1-3 wild-type mice. In whole-cell patch clamp measurements, neurons overexpressing podoplanin presented with markedly increased spontaneous synaptic activity as reflected by enhanced frequency of miniature excitatory postsynaptic currents (mEPSCs) when compared to neurons expressing GFP alone (Figure 5). Morphologically, podoplanin overexpression also induced the formation of a large number of short filopodial-like protrusions at the somatic region, a phenomenon not observed in neurons overexpressing the

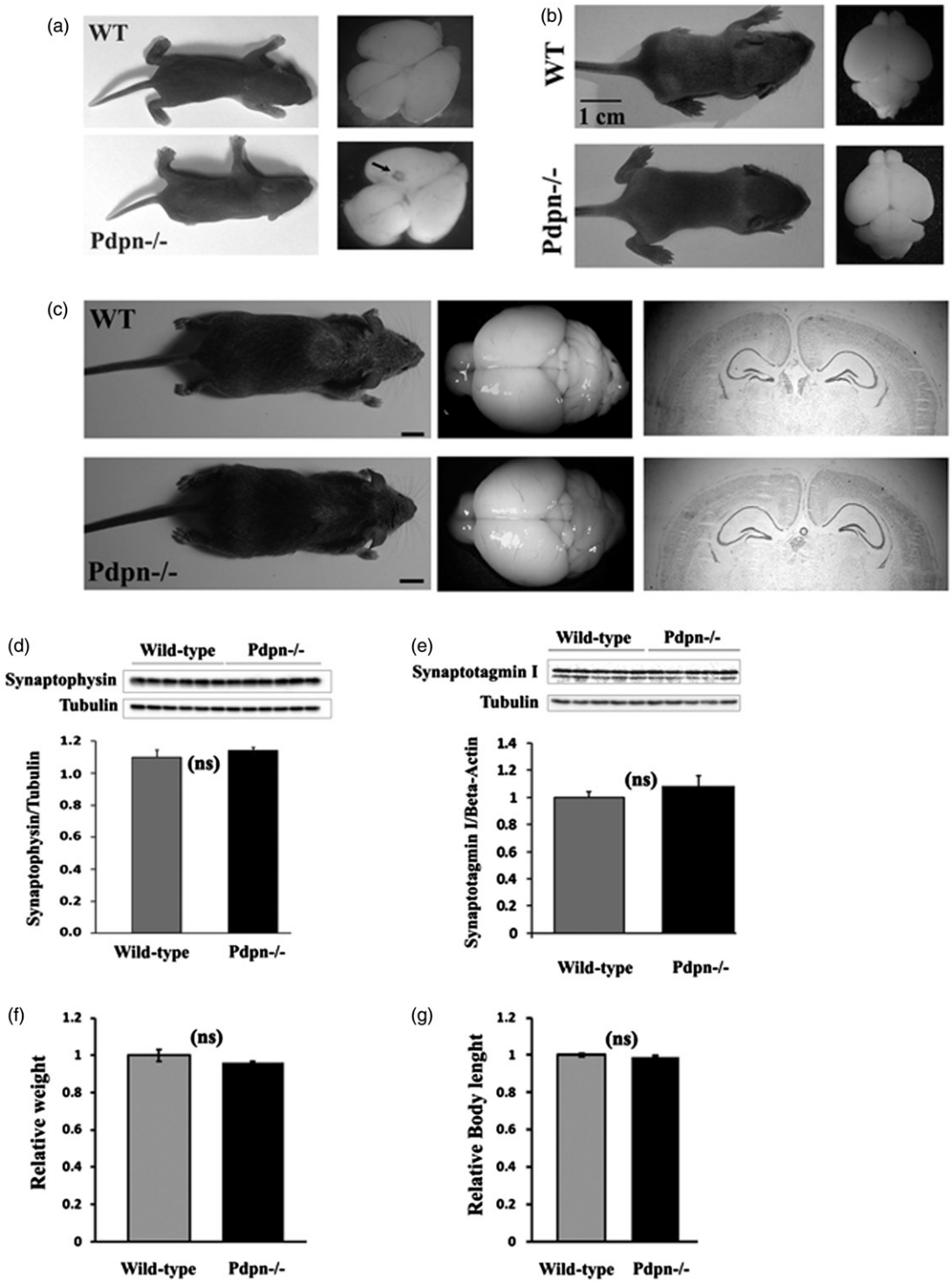

Figure 4. Survivor podoplanin−/− mice don't exhibit other distinctive phenotypic abnormalities. (a) Podoplanin−/− (Pdpn−/−) newborn mice (postnatal day PND1-3) presented without obvious differences in body (lower left) or brain (lower right) gross structural appearance compared to wild-type (WT) animals (upper left and right pictures, representative images from n = 4 animals per group analyzed). Small vessel morphology anomalies were observable in the cortex of some podoplanin−/− brains (arrow). (b) While body and brain morphology remained undistinguishable between wild-type and podoplanin−/− mice 10 days after birth (left pictures), vessel morphology anomalies were not any more visible in the brain of podoplanin−/− mice (right lower picture). (c) Also in mature adult mice, no apparent differences in body (left) and brain morphology (middle) and no vessel anomalies were observed for wild-type and podoplanin−/− mice (bars =1 cm). Stained brain coronal sections showed no obvious differences in shape and cytoarchitectonic organization for cortex, hippocampus or other structures for wild type and podoplanin−/− brains (right panels). (d) In adulthood, the levels of the synaptic proteins synaptophysin and synaptotagmin I (e), as well as physiological parameters including body weights (f) and body length (g) were also indistinguishable between wild-type and podoplanin−/− mice. ns ($p > 0.05$).

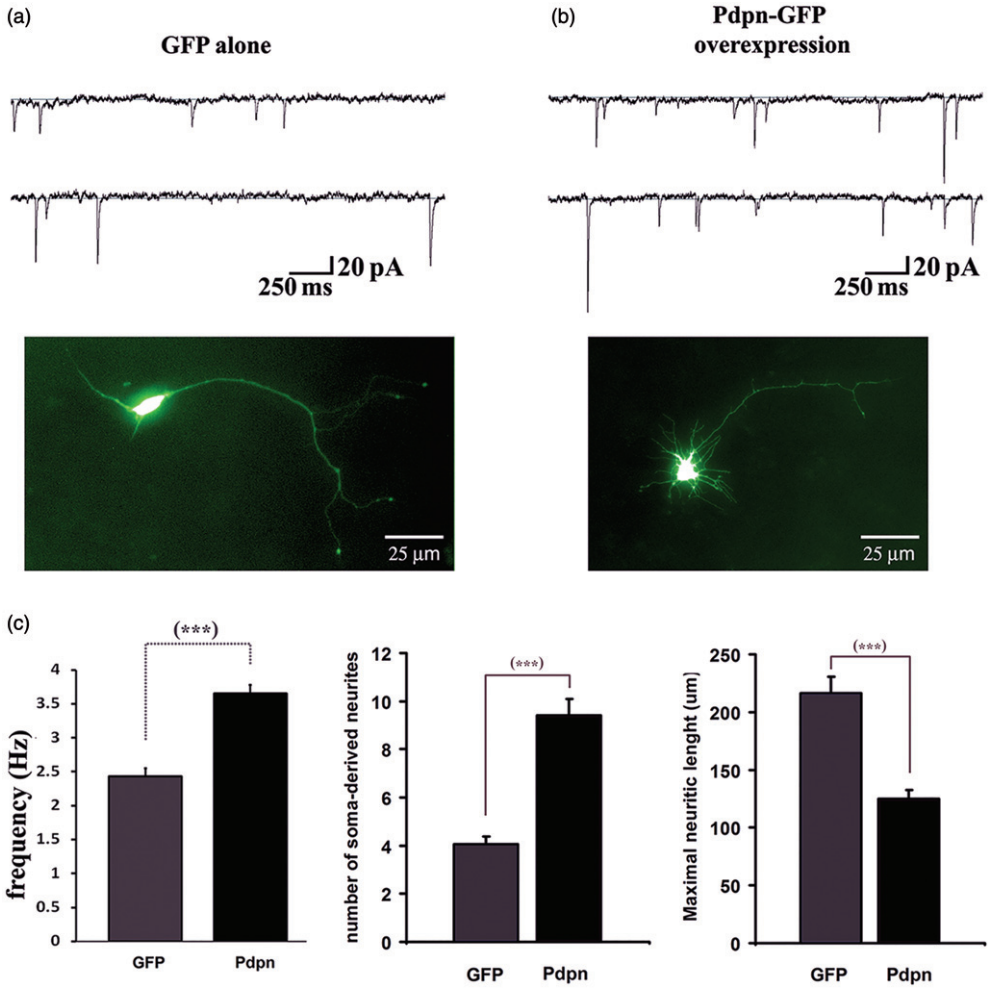

Figure 5. Podoplanin overexpression promotes synaptic activity and neuritic outgrowth. Hippocampal "sister" neurons from wild-type mice and cultured in identical conditions were transfected with a DNA plasmidic vector encoding for either the expression of the GFP alone (a) or with DNA encoding for a podoplanin-GFP fusion protein (b). Recordings of mEPSCs revealed a significant increase in the frequency of spontaneous synaptic events in neurons expressing podoplanin relative to those expressing GFP alone (representative current traces, upper panels a-b and bar graph, left in (c). Overexpressing of podoplanin also resulted in larger number of soma-derived neurites, which appeared shorter in length (pictures illustrating representative neurons, a-b lower panels, and bar graphs, middle and right in (c). Data are displayed as mean ± SEM. ***($p \leq 0.001$).

Green Fluorescent Protein (GFP) used as control (Figure 5). Of note, the somatic promotion of neuritic extensions described here upon podoplanin overexpression consistently resembled the long filopodial-like protrusions induced upon overexpression of podoplanin in HMC-1 cells described previously (29).

Neurons deficient in podoplanin exhibit reduced response to NGF

Next, we examined the patterns of neuritic outgrowth under basal conditions and in response to NGF in primary cultured hippocampal neurons from new-born PND1-3 wild-type controls and podoplanin−/− mice. Whereas hippocampal neurons from both wild-type and podoplanin−/− mice showed comparable neurite outgrowth under basal culture conditions, treatment with NGF was less effective ($p \leq 0.01$) in supporting neuritic outgrowth in neurons from podoplanin−/− than in neurons from wild-type mice (Figure 6(a,b)). These observations suggest that both podoplanin and NGF could mediate in hippocampal synaptic plasticity, and potentially neurogenesis, through cooperative signaling (13,30).

Surface plasmon resonance indicates a direct podoplanin-NGF interaction

As a first preliminary attempt to explore a potential translational and biological relevance of a possible molecular cross-talk between podoplanin and NGF, we explored whether human podoplanin and human NGF could physically interact *in vitro*. To this aim, we used SPR and followed protocols previously described for

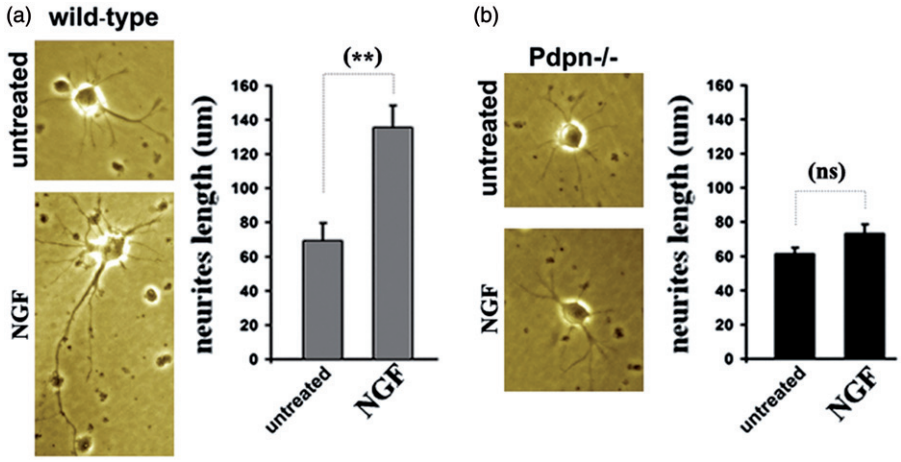

Figure 6. Podoplanin deletion hampers NGF-induced neuritic outgrowth. (a) Hippocampal neurons from wild-type mice developed observable neuritic extensions after three days in regular culture conditions (left). Neurites appear lengthened after three days of daily treatment with 50 ng/mL of NGF (middle). Right, bar graph comparison shows significant increase induced by NGF. (b) Hippocampal neurons from podoplanin−/− mice developed neuritic extensions comparable to those of wild-type after three days in regular conditions (left) but NGF treatment did not enhance neurite length (middle and right bar graph). Data are displayed as mean ± SEM. **($p \leq 0.01$), ns ($p > 0.05$).

the examination of podoplanin interactions with other proteins (31). SPR is one of the most widely used and recognized methods implemented for the study of quantitative binding affinities and kinetics for membrane proteins interacting with ligand molecules (32,33). SPR results yielded a K_d of about 100 nM for the interaction of NGF with immobilized podoplanin and showed a lack of interaction for the control peptide myostatin (GDF-8); thus, for the first time demonstrating a physical interaction between podoplanin and the neurogenic and memory-related brain neurotrophin NGF (Figure 7(a)). Since the protein Ezrin is expressed in brain neurons and has been shown to directly interact with podoplanin in non-neuronal cells, we also examined the effects of podoplanin depletion on the levels of Ezrin as well as its dependence on NGF stimulation in primary-cultured hippocampal neurons. No differences between wild-type and podoplanin−/− were observed for the basal levels of total Ezrin or phospho-Ezrin (p-Ezrin) (Figure 7(b,c)). However, upon NGF treatment (50 ng/mL/20 min), the levels of p-Ezrin in podoplanin−/− neurons were significantly lower ($p \leq 0.05$) than those from wild-type animals (Figure 7(d)). Similarly, while we did not observe differences between wild-type and podoplanin−/− neurons for basal levels of TrkA (Figure 7(e)), the treatment with NGF (50 ng/mL/2 h) significantly upregulated TrkA ($p \leq 0.01$) and CREB levels ($p \leq 0.05$) in neurons from wild-type mice and not in neurons from podoplanin−/− animals (Figure 7(f,g)).

The absence of differences in the basal levels of Ezrin, pEzrin, TrkA, and CREB between podoplanin−/− and wild type mice, in contrast to their response to NGF, suggests that adult podoplanin−/− mice do not exhibit a generalized pattern of neuronal phenotypic abnormalities but rather specific alterations in plasticity-related NGF signaling.

These data suggest the possible existence of a functionally relevant cross-talk between the NGF/TrkA and the podoplanin/Ezrin signaling pathways in the central nervous system.

Discussion

In this work, a podoplanin knockout mouse line that had been previously studied in the context of vascular physiology (12), as well as podoplanin-overexpression experiments, were used as a model to study the role of podoplanin in the mammalian brain neuron. Data obtained, comprises the first experimental evidence in support for an involvement of podoplanin in the promotion of neuritic outgrowth, synaptic activity, long-term synaptic plasticity, and *in vivo* hippocampus-dependent memory regulation. Additionally, this work proposes for the first time the existence of a functional crosst-alk between podoplanin and NGF, further supporting the hypothesis for a functional implication of podoplanin in the regulation of brain neuronal morphology.

This work also describes that although a large proportion of podoplanin knockout mice die after birth, yet a significant number of animals survive and reach adulthood lacking observable phenotypic abnormalities. This observation is consistent with previous reports (4,12) and suggests that some of the most salient phenotypic abnormalities resulting upon

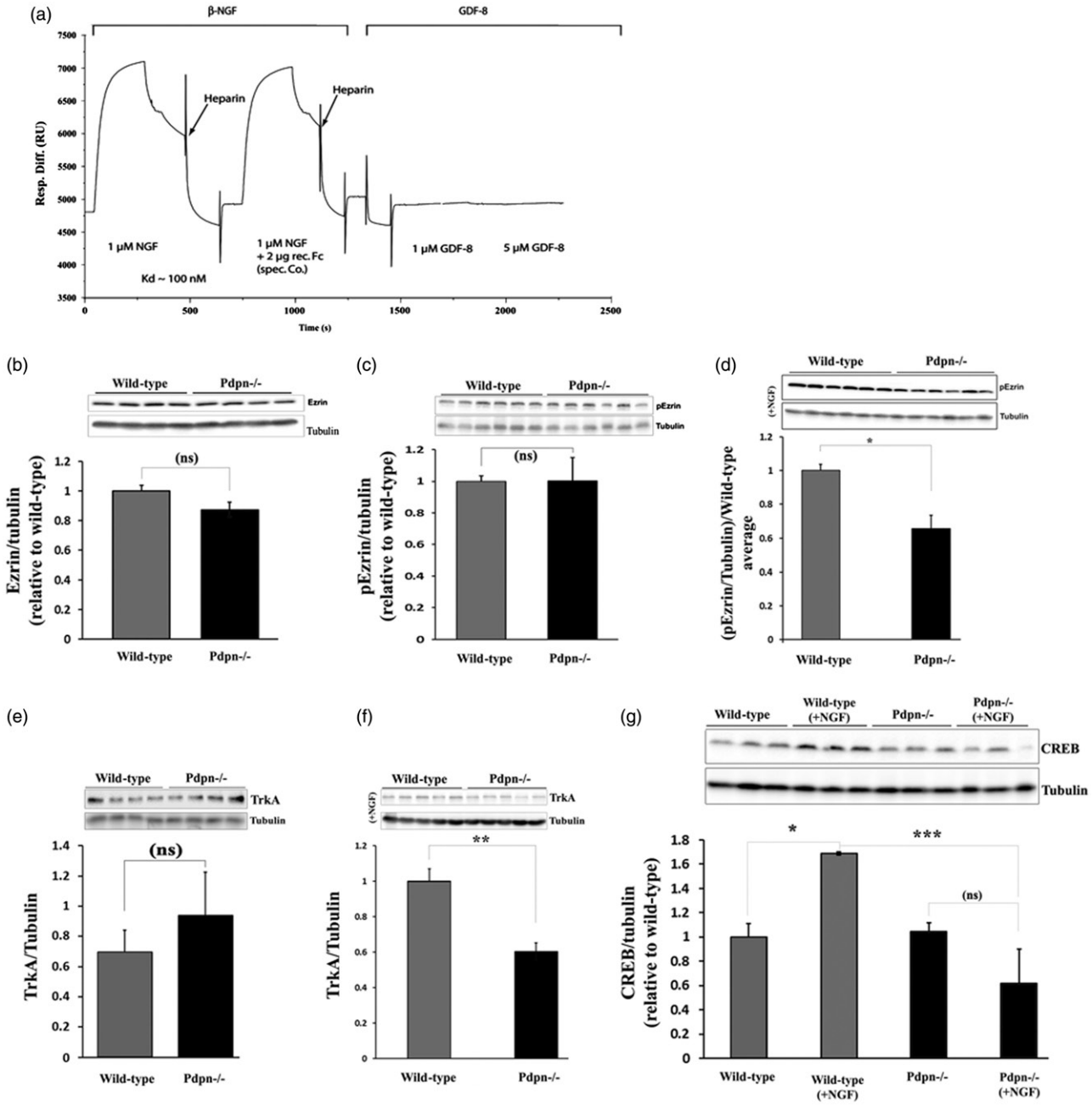

Figure 7. Podoplanin: a potential new player in the NGF/TrkA signaling pathway. (a) Real-time monitoring for potential human podoplanin and human NGF macromolecular interactions using SPR data obtained in a BiaCore apparatus showed a relatively high-affinity binding of recombinant NGF to immobilized podoplanin protein, as expressed in relative binding units on the y axis vs time. No binding was observed when a control GDF-8 recombinant protein was used even at concentrations five times higher than those used for the NGF assay. A heparin-based solution was used as a dissociation buffer. (b) No differences in the basal levels of total Ezrin or p-Ezrin (c) were observed between wild-type and podoplanin−/− mice hippocampal neurons. However, primary-cultured hippocampal neurons presented with comparatively lower levels of p-Ezrin upon NGF stimulation (50 ng/mL, 20 min) (d). Comparably, no differences in the levels of TrkA were observed under basal untreated conditions (e) but reduced levels were found in neurons from podoplanin−/− after NGF treatment (50 ng/mL, 2 h) (f). (g) Levels of CREB were also enhanced upon NGF stimulation in neurons from wild-type mice whereas CREB levels did not alter in response to NGF treatment in podoplanin−/− cultured neurons. Data are displayed as mean ± SEM. ns ($p > 0.05$), *($p \leq 0.05$), **($p \leq 0.01$), ***($p \leq 0.001$).

podoplanin genetic deletion can in some cases recede and resolve in the adulthood for biological reasons still undetermined. In agreement with this, no detectable effects on neuroarchitectural organization, levels of neuronal proteins, or other distinctive phenotypic abnormalities were observed here in adult animals lacking podoplanin. Paralleling descriptions of knockout mouse lines in which phenotypic abnormalities

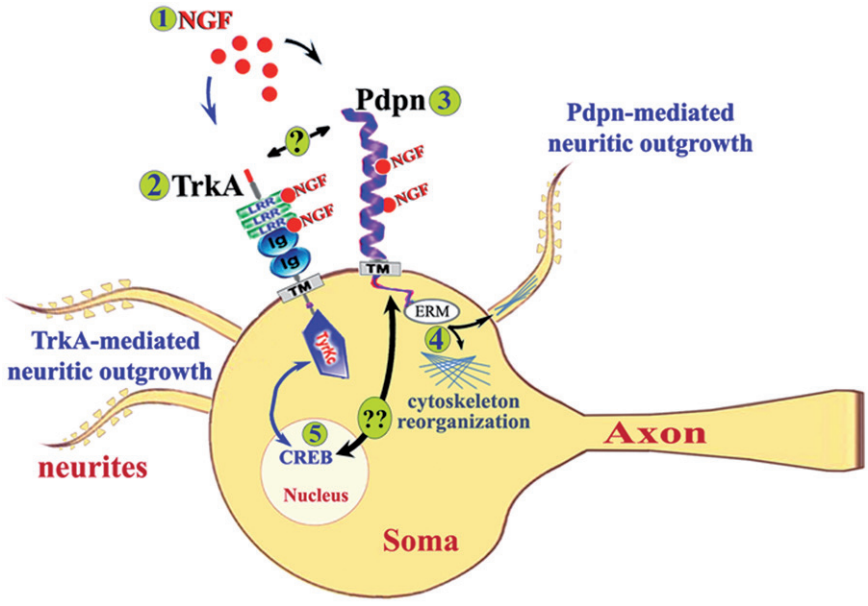

Figure 8. A proposed model for podoplanin signaling in the brain neurons. Extracellular NGF (1) binds to LRR or Ig-like domains of its canonical TrkA receptor (2) (it can also bind to p75 receptors not represented here) to induce well established CREB-mediated neuritic outgrowth important for synaptic plasticity and learning and memory. Concomitantly, extracellular NGF (1) can physically interact with podoplanin (3) to modulate podoplanin-related signaling via intracellular partners like Ezrin (4) to promote cytoskeleton reorganization and hence neuritic protrusion or retraction thus affecting the synaptic function. Whether podoplanin can also directly interact with TrkA receptors ("?" in the figure) thus affecting NGF/TrkA-mediated CREB signaling or whether podoplanin may, on its own ability, affect NGF-mediated CREB signaling (5) via a NGF/podoplanin signaling pathway ("??" in the figure) remains to be characterized.

recede with time have been described before (32). Moreover, although genetic deletion of podoplanin resulted in alterations of hippocampus-dependent memory storage, no effects on amygdala-dependent learning and memory functions were observed here, thus suggesting a brain region selective role for podoplanin in the modulation of activity-dependent neuroplasticity functions. Additionally, data presented here further propose a sub-region specificity for the involvement of podoplanin in plasticity-related functions, as podoplanin deletion selectively impaired synaptic function in the dentate gyrus without affecting the CA3-Schaffer Collateral-CA1 synapses, even though podoplanin is constitutively expressed in both hippocampal regions. Other groups have shown that alterations of hippocampus-dependent memory functions that are associated with disruptions in synaptic potentiation in the dentate gyrus can occur without detectable impairments in CA3-Schaffer Collateral-CA1 (21). These observations therefore suggest that podoplanin might have a type of sub-region specific activity that might rely on its potential interaction with molecules that have sub-region specific effects on hippocampal synaptic plasticity. Interestingly, a relevant cross-talk between podoplanin and NGF is proposed here and previous reports have described that NGF can promote memory-related synaptic plasticity specifically in dentate gyrus without affecting CA3-Schaffer Collateral-CA1 hippocampal synapses (13,33). NGF is a key regulator of hippocampal synaptic plasticity and memory functions (13). It may be therefore possible that some of the previously described selective effects of NGF on hippocampal synaptic plasticity imply a region-specific cross-talk between NGF and podoplanin. Moreover, NGF has also been previously associated to the function of CREB (34), which is critical for the maintenance of long-term memory storage (35). The significantly lower levels of both TrkA and the cyclic AMP response element binding protein (CREB) observed here upon stimulation with NGF in podoplanin−/− neurons, compared to wild-type neurons, support a potential involvement of podoplanin in the NGF signaling machinery (Figure 8), a hypothesis that still requires further examination in the physiological context.

A molecular player that could mediate the here proposed NGF-podoplanin cross-talk in the brain neuron is Ezrin, an interaction partner of podoplanin previously implicated in the regulation of morphology in non-neuronal cells (36–38). In agreement with this hypothesis, lower levels of phospho-Ezrin are reported here upon NGF stimulation of hippocampal neurons from podoplanin-deficient animals compared to those from wild-type mice. Interestingly, previous

experimental evidence has shown that the levels of Ezrin are regulated upon NGF stimulation in a TrkA-dependent manner and this NGF-dependent activation of Ezrin results in the remodeling of the growth cones of chick embryo dorsal root ganglia neurons (39). Our data therefore suggest that podoplanin might constitute a previously unidentified key molecular piece of the puzzle functionally linking the NGF/TrkA and the ERM protein family underlying neuronal filopodia formation and neuritogenesis in the mammalian nervous system (39–41).

For several years, two separated lines of evidence have independently related NGF (42–46) and podoplanin (4) to the promotion of malignant glioma proliferation. However, before this work, the possibility of a direct molecular cross-talk between podoplanin/Ezrin and the NGF/TrkA signaling pathway in the central nervous system has not been proposed to the best of our knowledge. Growing evidence continue supporting an implication of the NGF/TrkA signaling pathway in the pathophysiology of Alzheimeŕs disease (16–19), perhaps the most prevalent and devastating cause of progressive memory deterioration (47–52). In fact, novel clinical approaches specifically focus on the use of NGF as promising gene therapy for this neuropathology (47,53). However, to our knowledge, neither the relation of podoplanin to memory-related neuronal functions nor its direct biochemical interaction with NGF had been previously established. Therefore, our work has the potential to bring together two previously disassociated molecular elements that might conjointly contribute to the brain function in health and disease.

Acknowledgements

We thank Mario Hilpert and Jarmila Uhrinova for help with plasmidic DNA amplifications; Robert Vilvoi for assistance with animal handling, and Sonali N. Reisinger for critical reading of the manuscript.

Disclosure statement

The authors report no conflicts of interest.

Funding

Ana Cicvaric, Jiaye Yang, Pavel Uhrin, and Francisco Monje were supported by the Austrian Science Fund [FWF: Project Number P_27551].

References

1. Nose K, Saito H, Kuroki T. Isolation of a gene sequence induced later by tumor-promoting 12-O-tetradecanoylphorbol-13-acetate in mouse osteoblastic cells (MC3T3-E1) and expressed constitutively in ras-transformed cells. Cell Growth Differ. 1990;1:511–18.
2. Wetterwald A, Hoffstetter W, Cecchini MG, Lanske B, Wagner C, Fleisch H, et al. Characterization and cloning of the E11 antigen, a marker expressed by rat osteoblasts and osteocytes. Bone. 1996;18:125–32.
3. Breiteneder-Geleff S, Matsui K, Soleiman A, Meraner P, Poczewski H, Kalt R, et al. Podoplanin, novel 43-kd membrane protein of glomerular epithelial cells, is down-regulated in puromycin nephrosis. Am J Pathol. 1997;151:1141–52.
4. Astarita JL, Acton SE, Turley SJ. Podoplanin: emerging functions in development, the immune system, and cancer. Front Immunol. 2012;3:283.
5. Yurrita MM, Fernandez-Munoz B, Del Castillo G, Martin-Villar E, Renart J, Quintanilla M. Podoplanin is a substrate of presenilin-1/γ-secretase. Int J Biochem Cell Biol. 2014;46:68–75.
6. Shimojo M, Sahara N, Mizoroki T, Funamoto S, Morishima-Kawashima M, Kudo T, et al. Enzymatic characteristics of I213T mutant presenilin-1/gamma-secretase in cell models and knock-in mouse brains: familial Alzheimer disease-linked mutation impairs gamma-site cleavage of amyloid precursor protein C-terminal fragment beta. J Biol Chem. 2008;283:16488–96.
7. Uemura K, Farner KC, Hashimoto T, Nasser-Ghodsi N, Wolfe MS, Koo EH, et al. Substrate docking to gamma-secretase allows access of gamma-secretase modulators to an allosteric site. Nature Commun. 2010;1:130.
8. Uemura K, Kuzuya A, Shimozono Y, Aoyagi N, Ando K, Shimohama S, et al. GSK3beta activity modifies the localization and function of presenilin 1. J Biol Chem. 2007;282:15823–32.
9. Xia D, Watanabe H, Wu B, Lee SH, Li Y, Tsvetkov E, et al. Presenilin-1 knockin mice reveal loss-of-function mechanism for familial Alzheimer's disease. Neuron. 2015;85:967–81.
10. Larrieu-Lahargue F, Welm AL, Bouchecareilh M, Alitalo K, Li DY, Bikfalvi A, et al. Blocking Fibroblast Growth Factor receptor signaling inhibits tumor growth, lymphangiogenesis, and metastasis. PLoS One. 2012;7:e39540.
11. Suzuki H, Kato Y, Kaneko MK, Okita Y, Narimatsu H, Kato M. Induction of podoplanin by transforming growth factor-beta in human fibrosarcoma. FEBS Lett. 2008;582:341–5.
12. Uhrin P, Zaujec J, Breuss JM, Olcaydu D, Chrenek P, Stockinger H, et al. Novel function for blood platelets and podoplanin in developmental separation of blood and lymphatic circulation. Blood. 2010;115:3997–4005.
13. Conner JM, Franks KM, Titterness AK, Russell K, Merrill DA, Christie BR, et al. NGF is essential for hippocampal plasticity and learning. J Neurosci. 2009;29:10883–9.
14. Brown MC, Staniszewska I, Lazarovici P, Tuszynski GP, Del Valle L, Marcinkiewicz C. Regulatory effect of nerve growth factor in alpha9beta1 integrin-dependent progression of glioblastoma. Neuro-Oncology. 2008;10:968–80.

15. Forsyth PA, Krishna N, Lawn S, Valadez JG, Qu X, Fenstermacher DA, et al. p75 neurotrophin receptor cleavage by α- and γ-secretases is required for neurotrophin-mediated proliferation of brain tumor-initiating cells. J Biol Chem. 2014;289:8067–85.
16. Hock CH, Heese K, Olivieri G, Hulette CH, Rosenberg C, Nitsch RM, et al. Alterations in neurotrophins and neurotrophin receptors in Alzheimer's disease. J Neural Transm Suppl. 2000;59:171–4.
17. Lad SP, Neet KE, Mufson EJ. Nerve growth factor: structure, function and therapeutic implications for Alzheimer's disease. Curr Drug Targets CNS Neurol Disord. 2003;2:315–34.
18. Lapchak PA. Nerve growth factor pharmacology: application to the treatment of cholinergic neurodegeneration in Alzheimer's disease. Exp Neurol. 1993;124: 16–20.
19. Rattray M. Is there nicotinic modulation of nerve growth factor? Implications for cholinergic therapies in Alzheimer's disease. Biol Psychiat. 2001;49:185–93.
20. Monje FJ, Kim EJ, Pollak DD, Cabatic M, Li L, Baston A, et al. Focal adhesion kinase regulates neuronal growth, synaptic plasticity and hippocampus-dependent spatial learning and memory. Neuro-Signals. 2012;20:1–14.
21. Massa F, Koehl M, Wiesner T, Grosjean N, Revest JM, Piazza PV, et al. Conditional reduction of adult neurogenesis impairs bidirectional hippocampal synaptic plasticity. Proc Natl Acad Sci USA. 2011;108:6644–9.
22. Kotani M, Tajima Y, Osanai T, Irie A, Iwatsuki K, Kanai-Azuma M, et al. Complementary DNA cloning and characterization of RANDAM-2, a type I membrane molecule specifically expressed on glutamatergic neuronal cells in the mouse cerebrum. J Neurosci Res. 2003;73:603–13.
23. Pollak D, Weitzdoerfer R, Yang YW, Prast H, Hoeger H, Lubec G. Cerebellar protein expression in three different mouse strains and their relevance for motor performance. Neurochem Int. 2005;46:19–29.
24. Corcoran KA, Donnan MD, Tronson NC, Guzman YF, Gao C, Jovasevic V, et al. NMDA receptors in retrosplenial cortex are necessary for retrieval of recent and remote context fear memory. J Neurosci. 2011;31:11655–9.
25. Pollak DD, John J, Bubna-Littitz H, Schneider A, Hoeger H, Lubec G. Components of the protein quality control system are expressed in a strain-dependent manner in the mouse hippocampus. Neurochem Int. 2006;49: 500–7.
26. Pollak DD, John J, Scharl T, Leisch F, Schneider A, Hoeger H, et al. Strain-dependent regulation of neurotransmission and actin-remodelling proteins in the mouse hippocampus. Genes Brain Behav. 2006;5:200–4.
27. Pollak DD, John J, Schneider A, Hoeger H, Lubec G. Strain-dependent expression of signaling proteins in the mouse hippocampus. Neuroscience. 2006;138: 149–58.
28. Pollak DD, Scharl T, Leisch F, Herkner K, Villar SR, Hoeger H, et al. Strain-dependent regulation of plasticity-related proteins in the mouse hippocampus. Behav Brain Res. 2005;165:240–6.
29. Schacht V, Ramirez MI, Hong YK, Hirakawa S, Feng D, Harvey N, et al. T1alpha/podoplanin deficiency disrupts normal lymphatic vasculature formation and causes lymphedema. EMBO J. 2003;22:3546–56.
30. Zhao M, Li D, Shimazu K, Zhou YX, Lu B, Deng CX. Fibroblast growth factor receptor-1 is required for long-term potentiation, memory consolidation, and neurogenesis. Biol Psychiat. 2007;62:381–90.
31. Kerjaschki D, Regele HM, Moosberger I, Nagy-Bojarski K, Watschinger B, Soleiman A, et al. Lymphatic neoangiogenesis in human kidney transplants is associated with immunologically active lymphocytic infiltrates. J Am Soc Nephrol. 2004;15:603–12.
32. Lowe KL, Finney BA, Deppermann C, Hagerling R, Gazit SL, Frampton J, et al. Podoplanin and CLEC-2 drive cerebrovascular patterning and integrity during development. Blood. 2015;125:3769–77.
33. Kang H, Schuman EM. Long-lasting neurotrophin-induced enhancement of synaptic transmission in the adult hippocampus. Science. 1995;267: 1658–62.
34. Cox LJ, Hengst U, Gurskaya NG, Lukyanov KA, Jaffrey SR. Intra-axonal translation and retrograde trafficking of CREB promotes neuronal survival. Nature Cell Biol. 2008;10:149–59.
35. Abel T, Kandel E. Positive and negative regulatory mechanisms that mediate long-term memory storage. Brain Res Brain Res Rev. 1998;26:360–78.
36. Martin-Villar E, Megias D, Castel S, Yurrita MM, Vilaro S, Quintanilla M. Podoplanin binds ERM proteins to activate RhoA and promote epithelial-mesenchymal transition. J Cell Sci. 2006;119:4541–53.
37. Fernandez-Munoz B, Yurrita MM, Martin-Villar E, Carrasco-Ramirez P, Megias D, Renart J, et al. The transmembrane domain of podoplanin is required for its association with lipid rafts and the induction of epithelial-mesenchymal transition. Int J Biochem Cell Biol. 2011;43:886–96.
38. Smith SM, Melrose J. Podoplanin is expressed by a sub-population of human foetal rib and knee joint rudiment chondrocytes. Tissue Cell. 2011;43:39–44.
39. Marsick BM, San Miguel-Ruiz JE, Letourneau PC. Activation of ezrin/radixin/moesin mediates attractive growth cone guidance through regulation of growth cone actin and adhesion receptors. J Neurosci. 2012;32:282–96.
40. Gonzalez-Agosti C, Solomon F. Response of radixin to perturbations of growth cone morphology and motility in chick sympathetic neurons in vitro. Cell Motil Cytoskeleton. 1996;34:122–36.
41. Olsson PA, Korhonen L, Mercer EA, Lindholm D. MIR is a novel ERM-like protein that interacts with myosin regulatory light chain and inhibits neurite outgrowth. J Biol Chem 1999;274:36288–92.
42. Vinores SA, Perez-Polo JR. Nerve growth factor and neural oncology. J Neurosci Res. 1983;9:81–100.
43. Marushige Y, Marushige K, Koestner A. Chemical control of growth and morphological characteristics of anaplastic glioma cells. Anticancer Res. 1989;9:1729–35.
44. Li QY, Yang Y, Zhang Y, Zhang ZJ, Gong AH, Yuan ZC, et al. Nerve growth factor expression in astrocytoma and cerebrospinal fluid: a new biomarker for prognosis of astrocytoma. Chin Med J (Engl). 2011;124:2222–7.

45. Zhang Z, Yang Y, Gong A, Wang C, Liang Y, Chen Y. Localization of NGF and TrkA at mitotic apparatus in human glioma cell line U251. Biochem Biophys Res Commun. 2005;337:68–74.
46. Singer HS, Hansen B, Martinie D, Karp CL. Mitogenesis in glioblastoma multiforme cell lines: a role for NGF and its TrkA receptors. J Neurooncol. 1999;45:1–8.
47. Tuszynski MH, Yang JH, Barba D, U HS, Bakay RA, Pay MM, et al. Nerve growth factor gene therapy: activation of neuronal responses in Alzheimer disease. JAMA Neurol. 2015;72:1139–47.
48. Terry Jr AV, Kutiyanawalla A, Pillai A. Age-dependent alterations in nerve growth factor (NGF)-related proteins, sortilin, and learning and memory in rats. Physiol Behav. 2011;102:149–57.
49. Calissano P, Matrone C, Amadoro G. Nerve growth factor as a paradigm of neurotrophins related to Alzheimer's disease. Develop Neurobiol. 2010;70:372–83.
50. Schindowski K, Belarbi K, Buee L. Neurotrophic factors in Alzheimer's disease: role of axonal transport. Genes Brain Behav. 2008;7:43–56.
51. Xu W, Weissmiller AM, White 2nd JA, Fang F, Wang X, Wu Y, et al. Amyloid precursor protein-mediated endocytic pathway disruption induces axonal dysfunction and neurodegeneration. J Clin Invest. 2016;126:1815–33.
52. Xu CJ, Wang JL, Jin WL. The emerging therapeutic role of NGF in Alzheimer's disease. Neurochem Res. 2016;41:1211–18.
53. Tuszynski MH, Thal L, U HS, Pay MM, Blesch A, Conner J, et al. Nerve growth factor gene therapy for Alzheimer's disease. J Mol Neurosci. 2002;19:207.